HHS Public Access

Author manuscript

Nat Methods. Author manuscript; available in PMC 2011 August 01.

Published in final edited form as:

Nat Methods. 2011 February ; 8(2): 139–142. doi:10.1038/nmeth.1552.

Simultaneous 2-photon calcium imaging at different cortical depths *in vivo* with spatiotemporal multiplexing

Adrian Cheng[1,2,3,4], **J. Tiago Gonçalves**[2,4], **Peyman Golshani**[2], **Katsushi Arisaka**[1], and **Carlos Portera-Cailliau**[2,3]

[1] Department of Physics and Astronomy, University of California Los Angeles, Los Angeles, California, USA

[2] Department of Neurology, David Geffen School of Medicine, University of California Los Angeles, Los Angeles, California, USA

[3] Department of Neurobiology, David Geffen School of Medicine, University of California Los Angeles, Los Angeles, California, USA

Abstract

In vivo 2-photon calcium imaging would benefit from the use of multiple excitation beams to increase scanning speed, signal-to-noise ratio, field of view, or to image different axial planes simultaneously. We adapted a spatiotemporal multiplexing approach to circumvent the problem of light scattering ambiguity in deep tissue inherent to multifocal 2-photon microscopy. We demonstrate 2-photon calcium imaging at multiple axial planes in the in vivo mouse brain to monitor network activity of large ensembles of cortical neurons in three spatial dimensions.

Keywords

Microscopy; Imaging; Neuroscience

Optical probing of neuronal activity with fluorescent calcium indicators is a powerful approach to study information processing in the brain[1]. In particular, calcium imaging with 2-photon laser scanning microscopy (2PLSM)[2] is an ideal tool for recording network activity *in vivo* because it is less invasive than electrophysiology, more cells can be monitored simultaneously, and one can identify the cells being recorded[3]. Recently, several approaches have been introduced to overcome the traditionally slow raster scanning in 2-photon calcium imaging (2PCI), including acousto-optic deflectors (AODs) or targeted path

Address correspondence to: Carlos Portera-Cailliau, UCLA Neurology, RNRC A-145, 710 Westwood Plaza, Los Angeles, CA 90095; CPCailliau@mednet.ucla.edu.

[4]These authors contributed equally to this work.

Author contributions: A.C., T.G., P.G., K.A., and C.P.-C. conceived the project. A.C. designed and built the microscope and control electronics, and developed the microscope software. T.G. performed *in vivo* multifocal calcium imaging and simultaneous cell-attached recordings. A.C. analyzed the data. A.C., T.G. and C.P.-C. wrote the manuscript. K.A. and C.P.-C. supervised the project.

COMPETING FINANCIAL INTERESTS

The authors declare no competing financial interest

scanning with closed loop scanning mirrors[5–7]. Thus, as better fluorescent probes and methods for enhancing excitation and detection become available, temporal resolution in 2PCI will improve further and reporting of action potential firing will be possible for large groups of neurons and volumes of tissue *in vivo*.

Another way to improve temporal resolution in 2PCI is to scan the sample with multiple beams in parallel[8–9]. In fact, because time resolution, signal to noise (SNR) and field of view (FOV) are closely related in 2PCI, multifocal scanning would lead to improvements in all of these areas. For instance, in cases where non-linear photodamage is a limitation[10], scanning with multiple beams simultaneously and increasing the rate at which laser pulses are delivered to the sample will increase SNR[11]. Importantly, another potential advantage of multifocal 2PLSM would be the capability to perform calcium imaging of multiple axial planes simultaneously.

Because the brain is a heterogeneous medium that greatly scatters and absorbs light, multifocal 2PCI in the intact brain has not yet been feasible at depths of > 100 μm. The deep-tissue imaging capability of 2PLSM requires non-descanned detection of scattered fluorescence[2], relying solely on excitation for spatial contrast. Existing commercial multifocal 2PLSM systems use cameras that generate spatial contrast through detection[8], which is subject to much greater scattering than excitation for a given depth[12]. This leads to a substantial loss of spatial resolution and signal strength with depth (Supplementary Fig. 1). The use of de-scanned detector arrays such as multi-anode photomultiplier tubes (PMTs) can decrease this effect[9], but this method is still subject to scattering ambiguity in the form of emission cross-talk and is limited to <70 μm tissue penetration.

A solution to the problem of extending multifocal raster scanning with 2PLSM to deep tissue is to use spatiotemporal excitation pulse multiplexing and demultiplexed readout[13]. The feasibility of this approach to image fluorescent samples at multiple focal planes has been demonstrated with custom lasers[13–15]. It was hypothesized that this method would allow multiple beams to be used in deep tissue without scattering ambiguity[14]. Here, we adopted this approach for 2PCI *in vivo* using traditional non-descanned detection to collect all scattered light and attribute it to individual beams. We demonstrate that this technique can be applied to achieve multifocal 2PCI in the intact mouse neocortex, at depths greater than the visible wavelength mean free path length and in multiple axial planes across several cortical layers.

Our multifocal 2PCI approach takes advantage of the shorter fluorescence decay time of synthetic fluorescent calcium indicator dyes (typically in the ns range) relative to the laser repetition periods (tens of ns) in order to interleave beams in time. This permits fluorescence from spatially distinct beams to be distinguished, because fluorescence detected at different times is assigned to different portions of the image (Fig. 1). The number of beams that can be implemented is ultimately determined by the laser repetition rate and the fluorophore's decay time Using astandard80 MHz Ti:Al_2O_3 laser, this translates into simultaneously scanning four beams that are separated in time by ~3 ns, which works well for the commonly used dye Fluo-4 (~1 ns lifetime; Supplementary Note). Many more beams could be added (and more fluorophores accommodated) by using methods to reduce the repetition

rate of commercial lasers (Supplementary Note). In order to achieve short beam spacing and analog readout, we used a prototype hybrid photodetector[16] with a short single-photoelectron pulse width and transit time spread (see Online Methods). Nevertheless, a variety of detection schemes could be used[15].

To test whether multifocal 2PLSM with excitation-emission multiplexing can be used for calcium imaging in the intact brain, we combined our 4-beam system with a resonant scanning mirror (although any scanning method could be used; Supplementary Note). This allows acquisition of 2-D images with 500 × 500 pixel resolution at up to 250 Hz, corresponding to a maximum field of view of ~400μm × 400μm using a 40× objective (Figs. 2 and 3, and Supplementary Fig. 2). We used standard Fluo-4 AM bulk loading protocols to record the activity of layer(L)2/3 neurons in the somatosensory cortex of isoflurane anesthetized mice. To identify cell contours for analysis, we used a morphological analysis of the time-dimension zero-lag cross-correlation image (Fig. 2b and Online Methods). For iterative identification of action potential-dependent calcium transients in neurons we used a 'peeling algorithm'[7], Online Methods), and constructed raster plots of discrete neuronal firing events (Fig. 2). Simultaneous patch-clamp recordings in cell-attached mode showed that the simulated calcium traces convolved from the electrophysiology recordings closely resembled the actual calcium traces (Supplementary Fig. 2). Thus, our prototype 4-beam time-multiplexed microscope performs well for *in vivo* 2PCI of the activity of L2/3 neurons, and provides the expected 4× larger FOV (or 4× greater time resolution) than conventional single beam 2PLSM systems.

A current limitation of 2PCI is that one cannot easily record network activity at different depths simultaneously. Using AODs with chirped acoustic signals, one can achieve inertia-less random-access axial focusing at kHz rates. However, 2PCI in multiple depths with AODs has only been demonstrated in brain slices with a modest ± 25 μm range[6]. The approach also requires four AODs, which introduces significant optical losses, as well as detrimental temporal and spatial dispersion. An alternative is to use a piezoelectric objective focusing unit to rapidly move the objective lens[5], which allows volumes to be scanned at rates of ~10 Hz, but the approach is ultimately inertia-limited. Importantly, neither method captures full imaging data, precluding the use of image registration methods for motion correction or image processing algorithms for cell detection a posteriori.

To image calcium signals in 3-D with spatiotemporal multiplexing, we implemented slight modifications in the optics of our system in order to scan separate imaging planes with different beams (Supplementary Fig. 3). Beams were arranged quasi-collinearly with a lens added for each beam to allow for focus offset in the axial direction while maintaining uniform back aperture filling. The beams were spaced 30 μm apart from each other in the z-axis for a total pitch of 90 μm. The total axial spacing is ultimately limited by spherical aberration of the objective lens (Supplementary Note). This allowed us to monitor the activity of ~100–200 neurons distributed over a cortical volume spanning from L1 to L3 (Fig. 2h–j).

As a demonstration of the potential applications of multifocal 2PLSM with spatiotemporal multiplexing, we conducted 2PCI experiments at multiple axial depths to determine whether

spontaneous activity within L2/3 of barrel cortex can spread in a columnar fashion, as previously reported[17]. We recorded neuronal activity with Fluo-4 AM in postnatal day (P) 15-P21 anesthetized mice. In order to maximize the number of L2/3 cells imaged, we arranged the beams such that only 2 planes (spaced at 50 μm pitch) were imaged simultaneously, each with 2 beams (Fig. 3). Next, we identified cells that participated in synchronous bursts of activity, previously referred to as peaks of synchrony[17] (see Online Methods). We also constructed activity-derived connectivity diagrams and plotted the distribution of peak correlation coefficients amongst pairs of cells in separate depths within L2/3 (Fig. 3d). We find that only a minority of these bursts had an axial (depth) and radial (lateral) spread that would be consistent with columnar connectivity (Fig. 3e) and the relationship between peak correlation coefficient and the axial spread (ΔR) of a cell pair was indistinguishable for cells in the same imaging plane or in different planes (Fig. 3f). These data suggest that spontaneous activity within L2/3 does not tend to propagate along columnar boundaries.

Ideally, one would like to introduce more than four beams and accommodate a wider variety of fluorophores, including those with longer lifetimes. The simplest solution is to use a laser with a lower repetition rate, while conserving average power (Supplementary Note). In practice, to be able to use a range of fluorescent dyes, beams should be spaced on the order of 10 ns apart, giving a maximum sample pulse rate and pixel rate of 100 MHz. This is a maximum rate at which information can be extracted by fluorescence emission from a region over which the returning fluorescence is scattered and diffused. Ultimately, the pulse energy required depends on tissue scattering, depth, wavelength, pulse width, focus quality, overall system optical transmission, non-linear photodamage, and on the fluorophore of interest; in our case, a pulse energy of 0.1 – 1 nJ after the objective lens was sufficient for *in vivo* 2PCI. Therefore, using a 5 MHz laser with ~2–3 W average power at 800 nm, imaging with 8–16 beams should be feasible for a wide variety of commonly used fluorophores.

In summary, we have applied a spatiotemporal multiplexing technique to address the fundamental limitation of deep tissue scattering ambiguity in multifocal 2PLSM. In addition to yielding a four-fold increase in frame rate or FOV, we demonstrate simultaneous *in vivo* 2PCI at up to 4 different cortical depths across ~100 μm. In the future, the introduction of additional beams and greater axial pitch will make it possible to record activity from an entire volume of neocortex. Additionally, multiplexed multifocal 2PLSM could be combined with AOD scanning or targeted path scanning (Supplementary Note). In parallel with improvements in excitation efficiency, electronics, light collection and detectors that result in higher SNR, multifocal 2PCI with multiplexing will allow neuroscientists to explore new questions regarding the spatiotemporal dynamics of neuronal activity over three spatial dimensions.

ONLINE METHODS

All chemicals were purchased from Sigma-Aldrich unless otherwise stated. All experiments were performed under animal protocols approved by the Animal Research Committee and the Office for the Protection of Research Subjects at the University of California, Los Angeles.

Spatiotemporal beam multiplexing

To construct the spatiotemporal beam multiplexing microscope prototype (Fig. 1a), we used simple optics to split the main beam from a 80 MHz Ti:Al_20_3 laser (Chameleon Ultra II, Coherent) into 4 spatiotemporally multiplexed beams. Polarizing beam splitters were used with half-wave plates to allow for varying power delivery via each beam. We calculated that, for a 3 ns delay between beams, each beam's path had to be extended by a distance of ~1 m. The delayed beams were then converged on a conjugate plane of the objective pupil at the desired angle. Differences in optical propagation time of emitted fluorescence due to each beam were deemed negligible due to the short differences in distance traveled (millimeters) compared to the optical delays (meters). Importantly, during fluorescence emission from each beam, the photodetector remains sensitive to the entire collection area of the objective, which ensures that the sensitivity and resolution are equivalent to those of a single beam system.

Pulse length is degraded by group delay dispersion (GDD) and, as determined by previous work[18] and by the Sellmeier equation, this is negligible for the optical train consisting of ~1 m air delay lines using several dielectric mirrors. The dominant contribution from delay lines is from dielectric mirrors (~20 fs^2 at 800 nm[18]). In the overall microscope system the largest contributors to GDD are the glass elements (506.0 fs^2/cm for BK7 glass at 800 nm, 594 fs^2/cm for LakL21 at 800 nm), and in comparison delay line dispersion is negligible.

For imaging different planes simultaneously, the beams were arranged quasi-collinearly with a lens added for each beam to allow for focus offset in the axial direction while maintaining uniform back aperture filling (Supplementary Fig. 3). Beams were spaced either 30 μm apart in the z-axis (for a total pitch of 90 μm) under 40× magnification in the case of four plane experiments (Fig. 2), 75 μm apart in the case of two plane experiments under 40× magnification, or 50 μm apart under 60× magnification (Fig. 3).

De-multiplexing fluorescence emission

In order to de-multiplex fluorescence emission, we chose a state-of-the-art hybrid photodetector (HPD; Hamamatsu Photonics), which uses an avalanche photodiode as an electron bombardment target instead of the dynode stages of a photomultiplier tube (PMT). The HPD has a high first stage electron bombardment gain, which allows a low excess noise factor (a measure of the charge fluctuation of each single photoelectron response) of ~1.3, as well as a high speed response (< 1 ns) that is limited by the capacitance of the target avalanche photodiode[19]. While the HPD's single photoelectron gain of approximately 10^5 is an order of magnitude lower than that of a PMT, the difference is recovered with a GHz preamplifier (Supplementary Fig. 4). The HPD we used has a GaAsP photocathode with a 3 mm diameter active area and 45% quantum efficiency at 510 nm. A custom circuit board was designed and fabricated to demodulate multiplexed signals, built around an analog multiplier integrated circuit (ADL5391, Analog Devices). Emission signals from the HPD were de-multiplexed by analog multiplication with 3 ns square pulses generated from the laser monitor signal. This results in four separate signals that are shaped and amplified for subsequent digitization. Thus, our prototype system has the capability to operate as a

fluorescence lifetime imaging system when used with a single excitation beam, using 3 ns wide gates in the time domain.

Laser scanning system, image display and storage

For calcium imaging with our prototype 4-beam system, we incorporated either a 16 kHz resonant scanning mirror (SC-30, EOPC) or a 12 kHz resonant scanning mirror (CRS, Cambridge Technology/GSI Lumonics). This is a conventional scan method that has been used previously for 2-photon laser scanning microscopy (2PLSM)[20–22]. The resonant scanning mirror executes a bidirectional sinusoidal scan, producing a line rate of 32 kHz or 24 kHz, respectively. We chose to compensate for the non-uniform power delivery per angle and depth with an electro-optic modulator (S-350, ConOptics), but one could instead block the edges of the scan range. For the slow scan axis we used a closed-loop scanning mirror (6200H, Cambridge Technology). Function generators were used to generate scanning mirror signals (33210A, Agilent). With these components, our 4-beam system is capable of acquisition rates of up to 250 frames per second with for 512 × 512 images for single plane imaging and 60 volumes per second for multiple plane imaging.

After de-multiplexing and amplification, signals were digitized by a standard four-channel frame-grabber acquisition board (Helios, Matrox; Supplementary Fig. 4). Using two HPDs and a fast analog switch (ZYSW-2-50DR, Mini-Circuits), two colors can be switched or interleaved at the pixel or frame level and digitized by the same board. Signal levels were digitized at 8-bit precision per sample at 80 MHz, using a clock signal derived from the laser. We did not use the HPD in a photon-counting read-out scheme to allow for high peak photon flux, but this is certainly possible. Once digitized, the data were transferred across the PCI-express peripheral bus at sustained transfer rates > 700 MB/s and then displayed in real time by custom software using supplied imaging libraries (Matrox Imaging Library, Matrox). Raw images were averaged for display purposes only (to help visualize Fluo-4 labeled cells), while complete raw data was stored on hard disk. Geometrical horizontal distortion due to sinusoidal scanning distortion was corrected offline by linear interpolation resampling, or online with nearest-neighbor resampling. Imaging data were stored across a custom-designed high-bandwidth hard disk array with a maximum sustained transfer rate of 400 MB/s (Windows XP, Microsoft). This allows for two channels of data to be recorded without interruption at roughly 100 MB/s at 10-bit resolution. Data can be continuously recorded until the disk array space is exhausted (~ 3 hours).

In vivo cranial window preparation, calcium dye injection and imaging

We used male and female juvenile c57Bl/6 mice (n = 12; postnatal days 15–21) for all experiments and followed standard protocols[23–25]. A modified cranial window surgery, in which the glass coverslip only partially covers the dura, leaving a gap for injecting the calcium indicator was performed under light isoflurane anesthesia (0.5–1% in O_2). Sulforhodamine (SR) 101 was also injected to label astrocytes. With 2–4 injections of the calcium dye per animal we can label thousands of L2/3 neurons over a large area (1 mm^2). 2-photon calcium imaging (2PCI) at 800 nm of Fluo-4 AM or Oregon green BAPTA-1 AM (OGB) began after a 30–60 min recovery period. We used three different objectives: 40× 1.0 NA (Zeiss), 40× 0.8 NA (Olympus) and 60× 0.9 NA (Olympus). Typically, an average

power of 1 W at 800 nm was input into the microscope (Supplementary Fig. 5). The emission of SR101 in the red channel (filter 629/53 nm) was separated from that of the calcium dye in a green channel (filter 525/50 nm) with a dichroic that transmits wavelengths above 562 nm. Calcium imaging was done under isoflurane anesthesia (~0.5–1%). Several 180 second image sequences were recorded (250 frames per second with 16 kHz resonant scanning mirror and single imaging plane; 60 volumes per second for four-plane imaging; and 100 volumes per second for two-plane imaging with 12 kHz resonant scanning mirror). For multiple plane imaging, individual beam powers were carefully adjusted by half-wave plates and polarizing beam splitters to compensate for varying depth of imaging and variations in preparations. Beam cross-talk due to fluorescence lifetime was deemed neglibible (Supplementary Figs. 6 and 7), and no losses due to multiple beam imaging were found (Supplementary Fig. 8).

Electrophysiological recordings

In vivo loose cell-attached recordings were performed as previously described[26], using a patch clamp amplifier (2400, A-M Systems, Sequim, WA) and borosilicate microelectrodes (4–6 MΩ) filled with a potassium gluconate solution containing (in mM) 105 K-gluconate, 30 KCl, 10 HEPES, 10 phosphocreatine, 4 ATP-Mg, 0.3 GTP (adjusted to pH 7.3 with KOH). Cells were targeted using the shadow-patch method[27].

Image processing and data analysis

Image processing was done using the MATLAB environment (Mathworks). Images were first transformed using linear interpolation to correct for the sinusoidal resonant scanner trajectory. Contours of cells were detected by generating an image of the zero-lag cross correlation (or normalized standard inner product) between a 1 μm neighborhood and a 10 μm neighborhood[28–29]. The resulting image was thresholded to generate cell contours. Once cells were identified, raw fluorescence intensity traces were calculated for each, and linear drift was then subtracted. A peeling algorithm[30] was applied to identify transients by procedurally fitting exponentials with fixed decay length of 1 s and amplitude at least 5% $\Delta F/F$ using linear least squares method, accepting fits with average R^2 improvement greater than 0.1 standard deviations over the mean. After each successful fit, the detected transient was subtracted from the data and another fit was attempted, until the end of the trace was reached. This resulted in lists of events, their amplitude, and times for each cell.

To identify peaks of synchrony, the event-amplitude was summed over all cells and a trigger was applied over time at a threshold determined by Monte Carlo analysis (n = 1,000 simulations), as previously described[31]. This consisted of generating Monte Carlo data sets assuming uniform event arrival time while preserving the event amplitude distribution and number, and then identifying the 95% CL threshold for peak total event amplitude per time. Once peaks of synchrony were identified, the spatial distribution of the cells participating in each peak was characterized using the standard deviation of cell position in the radial (i.e., lateral) and axial directions. To identify significantly correlated cell pairs, the peak of the cross correlation function between event rates for pairs of cells was calculated, as was the delay time at which the peak occurred (with a maximum amplitude of 1 s). Monte Carlo

analysis involving 1000 trials of randomly permuting of event times was performed to identify 95% CL thresholds for peak cross correlation values for each cell pair.

Supplementary Material

Refer to Web version on PubMed Central for supplementary material.

Acknowledgments

We thank D. Kleinfeld, J.F. Leger, and T. Otis, as well as members of the Portera-Cailliau laboratory for discussions and comments on the manuscript. We are also grateful to M. Suyama and Y. Kawai with Hamamatsu Photonics K.K. for engineering support. This work was supported by grants from the National Institutes of Health (the Eunice Kennedy Shriver National Institute of Child Health & Human Development and the National Institute of Neurological Disorders and Stroke).

References

1. Grewe BF, Helmchen F. Optical probing of neuronal ensemble activity. Curr Opin Neurobiol. 2009 S0959-4388(09)00125-1 [pii]. 10.1016/j.conb.2009.09.003
2. Svoboda K, Yasuda R. Principles of two-photon excitation microscopy and its applications to neuroscience. Neuron. 2006; 50:823–839. [PubMed: 16772166]
3. Kerlin AM, Andermann ML, Berezovskii VK, Reid RC. Broadly tuned response properties of diverse inhibitory neuron subtypes in mouse visual cortex. Neuron. 2010; 67:858–871. S0896-6273(10)00612-4 [pii]. 10.1016/j.neuron.2010.08.002 [PubMed: 20826316]
4. Kremer Y, et al. A spatio-temporally compensated acousto-optic scanner for two-photon microscopy providing large field of view. Opt Express. 2008; 16:10066–10076. 164908 [pii]. [PubMed: 18607414]
5. Gobel W, Kampa BM, Helmchen F. Imaging cellular network dynamics in three dimensions using fast 3D laser scanning. Nat Methods. 2007; 4:73–79. nmeth989 [pii]. 10.1038/nmeth989 [PubMed: 17143280]
6. Duemani Reddy G, Kelleher K, Fink R, Saggau P. Three-dimensional random access multiphoton microscopy for functional imaging of neuronal activity. Nat Neurosci. 2008; 11:713–720. [PubMed: 18432198]
7. Grewe BF, Langer D, Kasper H, Kampa BM, Helmchen F. High-speed *in vivo* calcium imaging reveals neuronal network activity with near-millisecond precision. Nat Methods. 2010; 7:399–405. nmeth.1453 [pii]. 10.1038/nmeth.1453 [PubMed: 20400966]
8. Nielsen T, Fricke M, Hellweg D, Andresen P. High efficiency beam splitter for multifocal multiphoton microscopy. J Microsc. 2001; 201:368–376. jmi852 [pii]. [PubMed: 11240852]
9. Kim H, et al. Mutlifocal multiphoton microscopy based on multianode photomultiplier tubes. Optics Express. 2007; 15:11658–11678. [PubMed: 19547526]
10. Hopt A, Neher E. Highly nonlinear photodamage in two-photon fluorescence microscopy. Biophys J. 2001; 80:2029–2036. S0006-3495(01)76173-5 [pii]. 10.1016/S0006-3495(01)76173-5 [PubMed: 11259316]
11. Ji N, Magee JC, Betzig E. High-speed, low-photodamage nonlinear imaging using passive pulse splitters. Nat Methods. 2008; 5:197–202. nmeth.1175 [pii]. 10.1038/nmeth.1175 [PubMed: 18204458]
12. Oheim M, Beaurepaire E, Chaigneau E, Mertz J, Charpak S. Two-photon microscopy in brain tissue: parameters influencing the imaging depth. J Neurosci Methods. 2001; 111:29–37. [PubMed: 11574117]
13. Amir W, et al. Simultaneous imaging of multiple focal planes using a two-photon scanning microscope. Opt Lett. 2007; 32:1731–1733. 138230 [pii]. [PubMed: 17572762]
14. Sheetz KE, Hoover EE, Carriles R, Kleinfeld D, Squier JA. Advancing multifocal nonlinear microscopy: development and application of a novel multibeam Yb:KGd(WO4)2 oscillator. Opt Express. 2008; 16:17574–17584. 172878 [pii]. [PubMed: 18958037]

15. Chandler E, et al. High-resolution mosaic imaging with multifocal, multiphoton photon-counting microscopy. Appl Opt. 2009; 48:2067–2077. 177670 [pii]. [PubMed: 19363544]
16. Michalet X, et al. Hybrid photodetector for single-molecule spectroscopy and microscopy. Proceedings of SPIE. 2008; 6862:0F1–0F12.
17. Cossart R, Aronov D, Yuste R. Attractor dynamics of network UP states in the neocortex. Nature. 2003; 423:283–288. nature01614 [pii]. 10.1038/nature01614 [PubMed: 12748641]
18. Beck M, Walmsley IA, Kafka JD. Group Delay Measurements of Optical-Components near 800 Nm. Ieee J Quantum Elect. 1991; 27:2074–2081.
19. Michalet X, et al. Hybrid photodetector for single-molecule spectroscopy and microscopy. Proceedings of SPIE. 2008; 6862:0F1–0F12.
20. Sanderson MJ, Parker I. Video-rate confocal microscopy. Methods Enzymol. 2003; 360:447–481. [PubMed: 12622163]
21. Fan GY, et al. Video-rate scanning two-photon excitation fluorescence microscopy and ratio imaging with cameleons. Biophys J. 1999; 76:2412–2420. [PubMed: 10233058]
22. Rochefort NL, et al. Sparsification of neuronal activity in the visual cortex at eye-opening. Proc Natl Acad Sci USA. 2009; 106:15049–15054. 0907660106 [pii]. 10.1073/pnas.0907660106 [PubMed: 19706480]
23. Mostany R, Portera-Cailliau C. A craniotomy surgery procedure for chronic brain imaging. J Vis Exp. 2008 680 [pii]. 10.3791/680
24. Golshani P, Portera-Cailliau C. *In vivo* 2-photon calcium imaging in layer 2/3 of mice. J Vis Exp. 2008 681 [pii]. 10.3791/681
25. Garaschuk O, Milos RI, Konnerth A. Targeted bulk-loading of fluorescent indicators for two-photon brain imaging *in vivo*. Nat Protoc. 2006; 1:380–386. nprot.2006.58 [pii]. 10.1038/nprot.2006.58 [PubMed: 17406260]
26. Golshani P, et al. Internally mediated developmental desynchronization of neocortical network activity. J Neurosci. 2009; 29:10890–10899. 29/35/10890 [pii]. 10.1523/JNEUROSCI.2012-09.2009 [PubMed: 19726647]
27. Kitamura K, Judkewitz B, Kano M, Denk W, Hausser M. Targeted patch-clamp recordings and single-cell electroporation of unlabeled neurons *in vivo*. Nat Methods. 2008; 5:61–67. nmeth1150 [pii]. 10.1038/nmeth1150 [PubMed: 18157136]
28. Smith SL, Hausser M. Parallel processing of visual space by neighboring neurons in mouse visual cortex. Nat Neurosci. 2010; 13:1144–1149. nn.2620 [pii]. 10.1038/nn.2620 [PubMed: 20711183]
29. Valmianski I, et al. Automatic identification of fluorescently labeled brain cells for rapid functional imaging. J Neurophysiol. 2010 jn.00484.2010 [pii]. 10.1152/jn.00484.2010
30. Grewe BF, Langer D, Kasper H, Kampa BM, Helmchen F. High-speed *in vivo* calcium imaging reveals neuronal network activity with near-millisecond precision. Nat Methods. 2010; 7:399–405. nmeth.1453 [pii]. 10.1038/nmeth.1453 [PubMed: 20400966]
31. Cossart R, Aronov D, Yuste R. Attractor dynamics of network UP states in the neocortex. Nature. 2003; 423:283–288. [pii]. 10.1038/nature01614nature01614 [PubMed: 12748641]

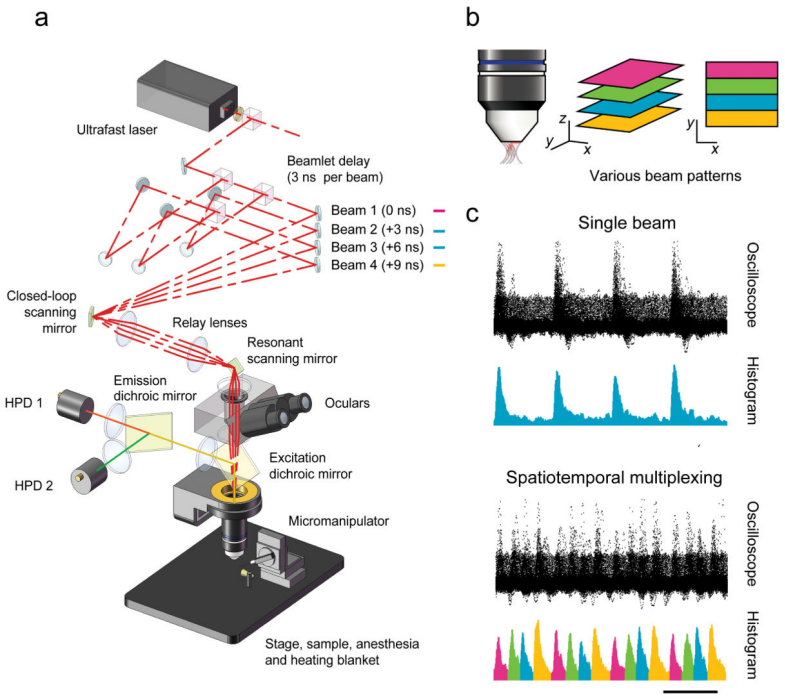

Figure 1.

Spatiotemporal multiplexing to overcome depth limitations in multifocal 2PLSM. (**a**) Layout of the prototype microscope. Laser pulses are emitted with 12 ns period from a commercial ultrafast Ti:Al_20_3 laser. The beam is divided into 4 beams, which are delayed by 3 ns each (1 m per 3 ns) and converged on the slow-axis scan mirror aperture, which is then projected onto the objective back aperture. The resulting emitted fluorescence, which is highly scattered, is collected by two hybrid photodetectors (HPDs). The HPD active area is placed in a demagnified conjugate plane of the objective back aperture to maximize scattered light collection. (**b**) Illustration of different beam scanning patterns at the sample. Time multiplexing removes ambiguity between different imaging planes, allowing both axial and lateral beam distribution. (**c**) Time course of detected fluorescence signal for a single beam (top) and four spatiotemporally multiplexed beams (bottom). Overlay of 200 oscilloscope traces and summary histograms of single photoelectron events (using a pollen grain). Fluorescence from different time windows (different colors) is associated with different delayed excitation beams. Scale bar: 12 ns.

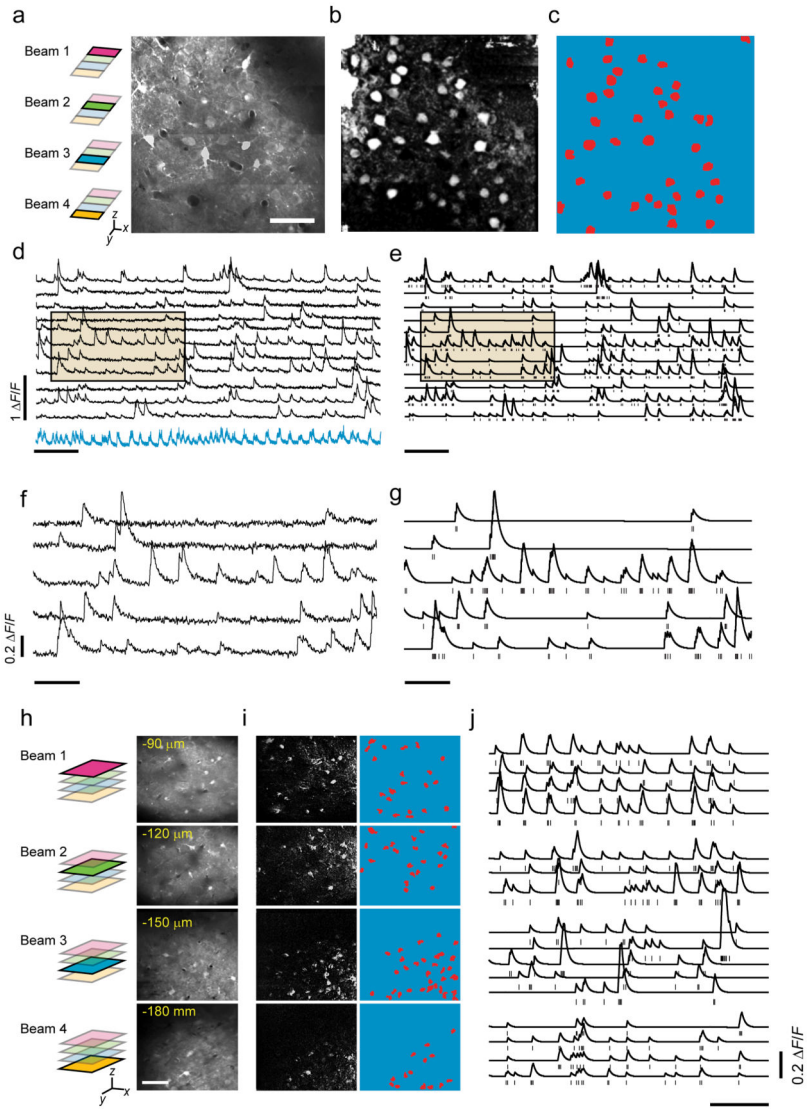

Figure 2.

Multifocal 2-D and 3-D *in vivo* 2-photon calcium imaging (2PCI) of L2/3 neurons in barrel cortex with spatiotemporal multiplexing. (**a**) Spatial distribution of four beams in a single image plane (left) and typical field of view (right). The image is an average intensity time projection of a representative calcium imaging movie (3 min, 250 frames per second) from a P20 mouse using Fluo-4AM. Scale bar: 50 μm.(**b**) Zero-lag cross-correlation image computed from the movie (see Online Methods). (**c**) Final segmented image of cell bodies obtained through morphological filters (red contours). (**d**) Raw calcium traces of 11 different cells (neuropil signal in blue). Scale bar: 20 s.(**e**) Model calcium traces with identified neuronal spiking events (tic marks) of selected cells using a peeling algorithm (see Online Methods). Scalebar: 20 s. (**f, g**) Details of shaded regions shown in **d** and **e,** respectively. Scale bar: 5 s. (**h**) Spatial distribution of four beams arranged axially (left) and field of view for each imaging plane (right). Images are average intensity time projections of a typical movie with Fluo-4 AM (3 min, 60 volumes per second) with depth spanning from 90 μm to

180 μm below the pia (encompassing L1 to L3). Scale bar: 50 μm. (**i**) Zero-lag cross-correlation image (left) and fully segmented image (right) with cell contours (red). (**j**) Selected traces reconstructed by the peeling algorithm (right). Scale bar: 20 s.

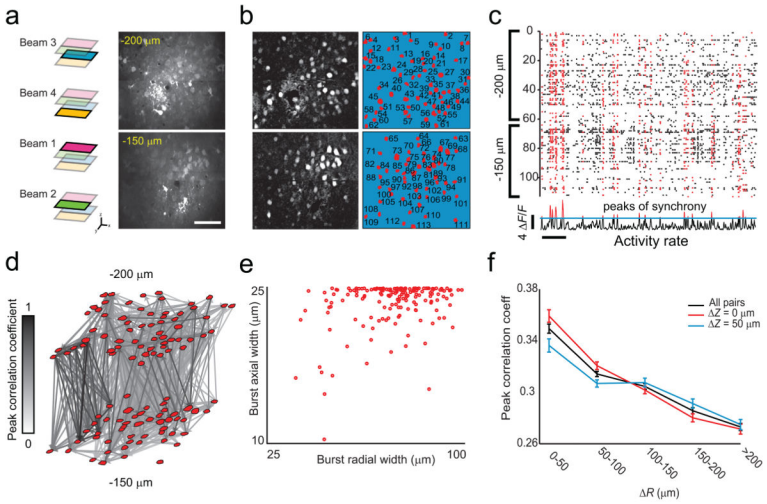

Figure 3.

Multifocal 2PCI with spatiotemporal multiplexing to assess activity-derived neuronal connectivity in L2/3 of barrel cortex. (**a**) Spatial distribution of four scanning beams (left) and representative field of view in two separate imaging planes (right) from an experiment with a P20 mouse using Fluo-4 AM (3 min, 100 frames per second). Scale bar: 50 µm. (**b**) Zero-lag cross-correlation image (left) and segmented image (right). (**c**) Raster plot showing identified spiking events in cells from **b**. Events shown in red were identified as having participated in a peak of synchrony (bottom trace). Scale bar: 20s.(**d**) Peak correlation coefficient (over a time lag of ± 1 s) for significantly correlated cells from **b**. (**e**) Axial (depth) versus radial (lateral) spread of bursts of neuronal firing corresponding to peaks of synchrony identified in several movies (n = 10 movies from 2 mice, n = 173 peaks of synchrony). A minority of bursts had a spatial organization consistent with either columnar (upper left) or laminar connectivity (bottom right). (**f**) Peak correlation coefficients from **c** versus cell pair radial distance (ΔR), for cell pairs in different imaging planes, the same imaging plane, and for all pairs (n = 10 movies, N = 10,262 pairs).